Simple and efficient decoupling of compact arrays with parasitic scatterers

Lau, Buon Kiong; Bach Andersen, Jørgen

Published in:
IEEE Transactions on Antennas and Propagation

DOI:
10.1109/TAP.2011.2173440

2012

Document Version:
Peer reviewed version (aka post-print)

Simple and Efficient Decoupling of Compact Arrays with Parasitic Scatterers

Buon Kiong Lau, *Senior Member, IEEE,* and Jørgen Bach Andersen, *Life Fellow, IEEE*

***Abstract*—Compact arrays such as multiple antennas on a mobile terminal suffer from low efficiency and high correlation between antenna signals. In the present paper, a simple and rigorous procedure for decoupling two closely coupled antennas with a parasitic scatterer is proposed. The parasitic scatterer, which can be an additional antenna, acts as a shield between two active antenna elements. In contrast to previous studies involving the use of parasitic scatterer for decoupling antennas, we demonstrate using antenna impedances the underlying decoupling mechanism for two arbitrary antennas. By a proper choice of parameters, perfect matching and decoupling can be obtained for a given antenna spacing without extending the overall area used, and without introducing additional decoupling networks. The price to pay is a reduction of bandwidth relative to that of widely spaced antennas, which is the case for other decoupling methods as well. Simulation and experimental results are used to substantiate the effectiveness of the proposed design approach on a two-monopole array with an antenna spacing of 0.1 wavelength. Finally, several practical considerations of the proposal are also presented, including the extension of the approach for more than two active antennas and its implementation in mobile terminals.**

***Index Terms*—Antenna array mutual coupling, parasitic antennas, impedance matching**

I. Introduction

CONVENTIONALLY, antenna arrays were used in radar installations and satellite communications. In these applications, it is typical to separate adjacent antenna elements by one half of a wavelength ($\lambda/2$), in order to maximize array resolution without the problem of ambiguity [3]. The same conclusions apply to the more recent application of antenna arrays at base stations in wireless communications (see *e.g.*, [4]).

However, the overall size of the array structure has become a subject of current interest, following the widespread adoption of multiple-input multiple-output (MIMO) technology in existing and future wireless communications standards [5]. One reason for this is that the implementation of multiple antennas in compact user terminals involves challenging design tradeoffs [6]. For example, even though techniques exist to mitigate mutual coupling and correlation among closely spaced antennas [6], the achievable bandwidth is reduced when compared to widely spaced antennas [7]. Nevertheless, antenna decoupling techniques can be used to facilitate a smaller antenna separation for a given set of performance requirements.

B. K. Lau is with the Department of Electrical and Information Technology, Lund University, Sweden, e-mail: bklau@ieee.org.

J. Bach Andersen is with the Department of Electronic Systems, Aalborg University, Denmark.

This work was financially supported by VINNOVA under grant no. 2008-00970 and Vetenskapsrådet under grant no. 2006-3012. This paper was presented in part at the International Workshop on Antenna Technology, Santa Monica, CA, Mar 2-4, 2009 [1] and also in part as a patent application [2].

Manuscript received June X, 2010.

A. Existing Decoupling Techniques

One well-studied technique to decouple closely spaced antennas is to apply the so-called multiport conjugate (MC) match through introducing a separate impedance matching network [6]–[15]. The MC match has been successfully demonstrated for monopoles [8], [10], [11], [13], [14], dipoles [7], [9], patch antennas [12] and planar inverted F antennas (PIFAs) [15]. Two drawbacks with implementing an additional network to achieve decoupling are that ohmic losses are expected from the decoupling network [14] and that the decoupling network can increase the overall footprint of the multiple antenna system. Other decoupling techniques, which are specific to antennas on a common ground plane, include ground plane modifications [16], [17] and use of neutralization line [18], [19].

More recently, the use of a parasitic element has been proposed as an attractive alternative to decouple two closely spaced antennas [20]–[23]. Akin to the MC match, it can decouple different types of antennas, including dipoles [20], [23], monopoles [21], [24], PIFAs [20], [24] and ultrawideband (UWB) antennas [25]. In fact, the use of parasitic elements in an antenna system is not new. Their previous applications, which are unrelated to decoupling of multiple antennas, include:

- changing of antenna patterns [26]–[30].
- limiting current flow of antenna on a small ground plane [31].
- enhancing bandwidth of the antenna structure [32]–[35].
- adding a resonant frequency band [36].
- increasing the reflection phase range of reflectarrays to beyond 360° [37].

One common feature in the existing literature on parasitic decoupling is that the design procedure minimizes the coupling coefficient in a best effort manner through sweeping the parameters of the parasitic element. As such, they are unlike the MC match, which generates perfect decoupling at the desired frequency for the given self and mutual impedances of the closely coupled antennas. Another commonality of existing parasitic decoupling literature, with the exception of [24], is that the structure of the parasitic element does not resemble that of the closely coupled antennas. For example, [20] proposes a H-shape structure and a meander T-shape

structure for decoupling dipoles and PIFAs, respectively, and a parameter sweep is employed to design these structures.

B. Proposed Parasitic Decoupling Technique

In this paper, we propose a simple and efficient parasitic decoupling technique, which can perfectly decouple two arbitrarily spaced antennas using a reactively loaded parasitic antenna in between them. It will be shown that our approach gives similar result as a MC matching network, but in a much simpler realization while maintaining the overall size of the antenna system. The proposed design procedure is simple and rigorous, in that the objective is to tune the dimensions of both the active and parasitic antennas in order to satisfy a criterion derived from antenna impedances. The criterion provides perfect decoupling of the active antennas through the use of a purely reactive load at the parasitic antenna. The reactive load ensures lossless decoupling in the case of ideal elements. Experimental results also show that the proposed technique gives significantly better measured efficiency than the MC match for two monopoles of 0.1λ spacing [13].

Whereas [24] shows the possibility to decouple two active antennas by placing a reactively loaded parasitic antenna in between them, it relies on numerical optimization of only the reactive load. No explicit information is provided on the underlying principle and mechanism, apart from the observation that loading the parasitic antenna with different reactive loads changes the gain patterns and coupling between the active antennas. In this paper, we show that tuning the active and parasitic antennas by changing their dimensions is necessary for achieving perfect decoupling at the center frequency.

The drawback of using any of the aforementioned techniques for coupling compensation is the narrow bandwidth of the resulting antenna system, but this is unavoidable for antenna systems with small antenna spacing [6]. Another consequence of these approaches is a change of radiation pattern, but this should only pose a minor problem in a rich scattering environment [38], and in fact it is angle diversity which facilitates the decorrelation of the signals. A simpler solution with optimum uncoupled port matching [39]–[41] is also a possibility, but the efficiency is reduced compared with decoupling techniques. The use of parasitic scatterer or reflector to increase isolation of UWB antennas (see [25] and references therein) has also been proposed. It is expected that a similar approach can be devised to enhance the bandwidth of decoupled narrowband antennas by generating multiple resonances in the parasitic element.

For the purpose of demonstrating the effectiveness of our parasitic decoupling concept and giving insight into its operation, we use electrical dipoles or monopoles as generic examples in this paper. However, the basic principle will work for any antenna, since the method only relies on antenna impedances.

The paper is organized as follows: Section II introduces the theoretical derivation of parasitic decoupling and the design procedure, which is illustrated using the simple case of two closely coupled dipoles. Section III shows the design approach for monopole antennas in full wave simulations, and the results are also verified in an experiment. Insights and practical issues relating to the technique are discussed in Section IV. Section V concludes the paper.

II. Theory of Decoupling with a Parasitic Scatterer

A. Derivation of Decoupling Procedure

The theory of decoupling two arbitrary active antennas with a parasitic scatterer can be illustrated with the setup in Fig. 1. The "black box" in the setup consists of two active antennas (ports 1 and 3) and a parasitic scatterer (port 2) that acts as a shield between the active antennas. The 3-port black box (or network) of multiple antennas is also intended to highlight the fact that the closely coupled antenna and scatterer cannot be considered as separate structures in general, *e.g.*, they may share a common ground. The parasitic scatterer is terminated by the load impedance Z_{L} and the matching circuits (or matching network) connected to antennas 1 and 3 transform the antenna input impedance to the impedance of the feed cable (typically 50Ω).

The self and mutual impedances of the three-port array at the center frequency f_0 ($f_0 = c/\lambda$, c being the speed of light in vacuum) are represented by Z_{ii} and Z_{ij}, respectively, where $i \neq j, \{i,j\} = 1,2,3$. We begin with the voltage and current relationship of the setup

$$\begin{bmatrix} V_1 \\ V_2 \\ V_3 \end{bmatrix} = \begin{bmatrix} Z_{11} & Z_{12} & Z_{13} \\ Z_{21} & Z_{22} & Z_{23} \\ Z_{31} & Z_{32} & Z_{33} \end{bmatrix} \begin{bmatrix} I_1 \\ I_2 \\ I_3 \end{bmatrix}, \tag{1}$$

or in matrix notation $\mathbf{V} = \mathbf{Z}_{\mathrm{A}}\mathbf{I}$, where V_i and I_i are the voltage and current across the ith antenna port. Moreover, due to reciprocity, $Z_{12} = Z_{21}$, $Z_{23} = Z_{32}$ and $Z_{13} = Z_{31}$.

The termination condition for the parasitic scatterer implies that $V_2 = -Z_{\mathrm{L}}I_2$, which upon substitution into (1) and rearrangement gives the voltage and current relationships across the ports of the active antennas

$$\begin{bmatrix} V_1 \\ V_3 \end{bmatrix} = \begin{bmatrix} Z'_{11} & Z'_{13} \\ Z'_{13} & Z'_{33} \end{bmatrix} \begin{bmatrix} I_1 \\ I_3 \end{bmatrix}, \tag{2}$$

where

$$Z'_{11} = Z_{11} - \frac{Z_{12}^2}{Z_{22} + Z_{\mathrm{L}}}, \tag{3}$$

$$Z'_{13} = Z_{13} - \frac{Z_{12}Z_{23}}{Z_{22} + Z_{\mathrm{L}}}, \tag{4}$$

$$Z'_{33} = Z_{33} - \frac{Z_{23}^2}{Z_{22} + Z_{\mathrm{L}}}. \tag{5}$$

To perfectly decouple the active antennas, we require that $Z'_{13} = 0$, or equivalently

$$Z'_{13} = Z_{13} - \frac{Z_{12}Z_{23}}{Z_{22} + Z_{\mathrm{L}}} = 0$$

$$\Rightarrow Z_{\mathrm{L}} = \frac{Z_{12}Z_{23}}{Z_{13}} - Z_{22}. \tag{6}$$

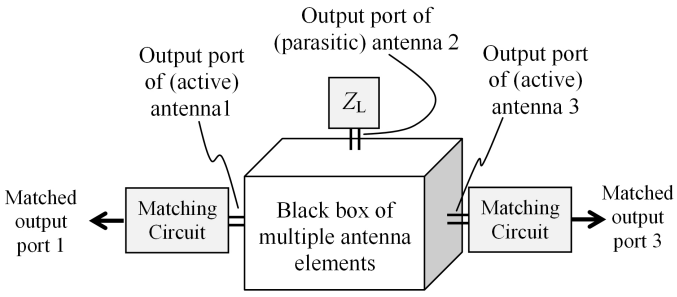

Fig. 1. A decoupling setup for a black box containing an arbitrary two-antenna structure (ports 1 and 3) and a parasitic scatterer (port 2). Port 2 is terminated with an impedance load, whereas each of ports 1 and 3 is matched to a 50Ω feed cable.

Treating the real $\mathrm{Re}\{\cdot\}$ and imaginary $\mathrm{Im}\{\cdot\}$ parts of (6) separately, and setting the load resistance to zero which will ideally circumvent any ohmic loss in the loaded scatterer

$$R_{\mathrm{L}} = \mathrm{Re}\{Z_{\mathrm{L}}\} = \mathrm{Re}\left\{\frac{Z_{12}Z_{23}}{Z_{13}}\right\} - R_{22} = 0, \tag{7}$$

$$X_{\mathrm{L}} = \mathrm{Im}\{Z_{\mathrm{L}}\} = \mathrm{Im}\left\{\frac{Z_{12}Z_{23}}{Z_{13}}\right\} - X_{22}, \tag{8}$$

where $R_{22} = \mathrm{Re}\{Z_{22}\}$ and $X_{22} = \mathrm{Im}\{Z_{22}\}$.

Based on the above derivation, the design procedure for decoupling can be formulated into the following steps:

1) For a given closely coupled two-antenna array, insert a third antenna between them as the parasitic scatterer.
2) Tune the three antennas so that criterion (7) is satisfied.
3) Calculate the reactance load Z_{L} for the parasitic scatterer using (8).
4) Calculate the new input impedances of the active antennas Z'_{11} and Z'_{33} using (3) and (5), respectively.
5) Calculate the required matching circuits to transform Z'_{11} and Z'_{33} to 50Ω.

B. Illustrative Example of Design Procedure

Since the above derivation is purely based on antenna impedances, the two antennas and the parasitic scatterer can be arbitrary and need not be of the same type. However, the commonly used reference of dipole antennas are used to demonstrate the decoupling procedure in the following numerical example. The setup is given in Fig. 2, which is identical to Fig. 1, except that the antennas are now explicitly shown. The center frequency is 900 MHz and the diameter of the dipoles is 2 mm. For simplicity, the dipole lengths are assumed to be identical $L = L_1 = L_2 = L_3$, such that $Z_{11} = Z_{22} = Z_{33}$ (*i.e.*, valid for the thin dipoles used here). In general, allowing for different lengths will increase the flexibility of the design method. The method-of-moments (MoM) Matlab scripts from [42] are used to generate the antenna impedances. The spacing between the two active dipoles is set at $d = 0.1\lambda$.

For this example, the criterion (7) can be achieved by adjusting the identical length of the dipole antennas L. As illustrated in Figure 3(a), two solutions satisfy this criterion, *i.e.*, $L = \{0.37\lambda, 0.48\lambda\}$ and the corresponding load reactances in Figure 3(b) are $X_{\mathrm{L}} = \{103.8\Omega, 19.9\Omega\}$. Therefore, the proposed procedure can in theory achieve perfect and lossless decoupling, *i.e.*, the scattering (or S) parameters $S'_{13} = S'_{31} = 0$, by ensuring that both conditions (7) and (8) are fulfilled. The reactive load at the parasitic element may be realized by either lumped (*e.g.*, inductor) or distributed (*e.g.*, open-circuited transmission line) elements. In this example, lossless inductors are used.

In general, the identical input impedance of dipoles 1 and 3 is not equal to the reference impedance of 50Ω when the load reactance of antenna 2 is set to one of the two values $X_{\mathrm{L}} = \{103.8\Omega, 19.9\Omega\}$. It follows from (3) and (6) that

$$Z'_{11} = Z_{11} - \frac{Z_{12}Z_{13}}{Z_{23}}, \tag{9}$$

which in this case reduces to

$$Z'_{11} = Z_{11} - Z_{13}, \tag{10}$$

due to the symmetry $Z_{12} = Z_{23}$.

The expression (10) implies that at the center frequency, the input impedance of the active antennas decreases correspondingly when the spacing d is reduced, due to the self and mutual impedances approaching each other. Therefore, if d becomes small, the required impedance transformation ratio to achieve 50Ω is high. For this example of $d = 0.1\lambda$, the input impedance of each of the two decoupled active port Z'_{11} are as low as $2.7 - j121.7\Omega$ and $5.9 + j11.9\Omega$, respectively, for the two solutions with $X_{\mathrm{L}} = \{103.8\Omega, 19.9\Omega\}$. This complicates the matching and gives narrowband results. However, it is possible to use a more sophisticated matching network (such as a Chebyshev design) to enhance the bandwidth of $S'_{11} = S'_{33}$ by more than a factor of two, if required, using a similar approach as for matching single antennas [43].

The impedance matching circuit needed to transform the impedance of each of the two decoupled active antennas (*i.e.*, Z'_{11} and Z'_{33}) to 50Ω is realized here with transmission lines and a single open-circuited stub [44], although lumped elements [44] may be more attractive for circuit miniaturization, especially at lower frequencies. Note that similar uncoupled matching circuits are required for any realization of MC match, except that in the present case the decoupling function of the decoupler line [10] or the rat-race hybrid $180°$ coupler [11] in the overall MC matching circuit is provided by the parasitic scatterer.

The scattering parameters of the decoupled active antennas using either of the two reactance load solutions are shown in Figure 4, where S'_{11} and S'_{13} are the scattering parameters of the active antennas after the decoupling *and* 50Ω matching steps. Lossless inductors are used in the MoM simulation to provide the required reactance load at the parasitic scatterer. As expected, perfect decoupling and matching is achieved at the center frequency for either of the two solutions. However, the solution with the shorter dipoles gives a more narrowband behavior in S'_{11}, as can be expected from the higher reactance load needed. As a reference case, the scattering parameters of two half-wavelength dipoles that are individually conjugate matched with their self-impedances (*i.e.*, self impedance match) are also shown. In this case, the antenna spacing of 0.1λ is kept and no parasitic scatterer is used. Comparing the

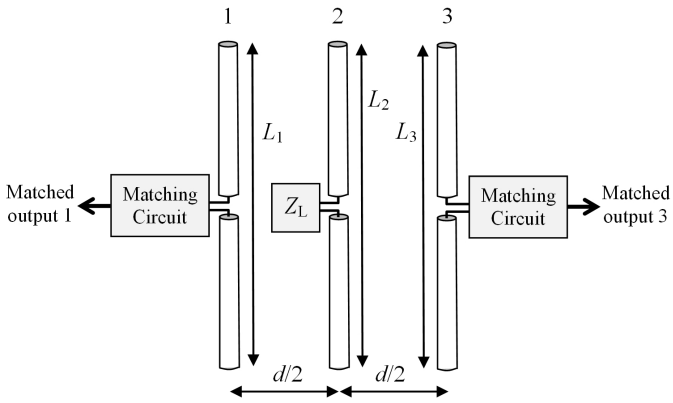

Fig. 2. A decoupling setup with the dipole 2 acting as a parasitic scatterer for the active dipoles 1 and 3. The parasitic scatterer is terminated with an impedance load.

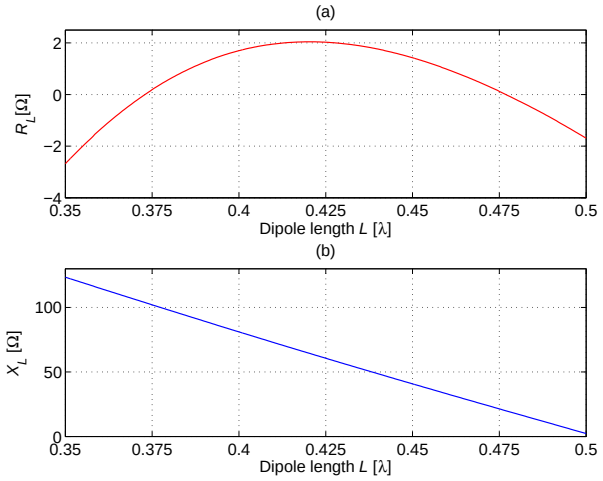

Fig. 3. Load (a) resistance and (b) reactance of the parasitic scatterer for perfect decoupling versus the length of the dipole antennas.

decoupling case with the reference case, it is clear that the decoupling approach gives very good matching performance, albeit for a relatively small bandwidth.

As another comparison, the scattering parameters for a realization of MC match based on hybrid 180° coupler [11], [13] are also provided in Figure 4. Using this realization, the output ports contain the odd and even modes. The isolation between the odd and even modes has a large bandwidth and thus not shown here. As in the reference case, the antenna spacing is 0.1λ and no parasitic scatterer is used. It is observed that the odd mode of the MC match, which has a smaller bandwidth than the even mode, has been found to yield similar bandwidth performance to the $L = 0.48\lambda$ solution of the parasitic decoupling approach.

III. Simulation and Experimental Verification

In this section, we present simulation and experimental results of the proposed decoupling approach at 900 MHz for the monopole antenna setup shown in Fig. 5. The same monopole array structure as in [40] is used, except that here we use three monopoles, instead of only two. Monopole 2 is the parasitic scatterer, whereas monopoles 1 and 3 are the

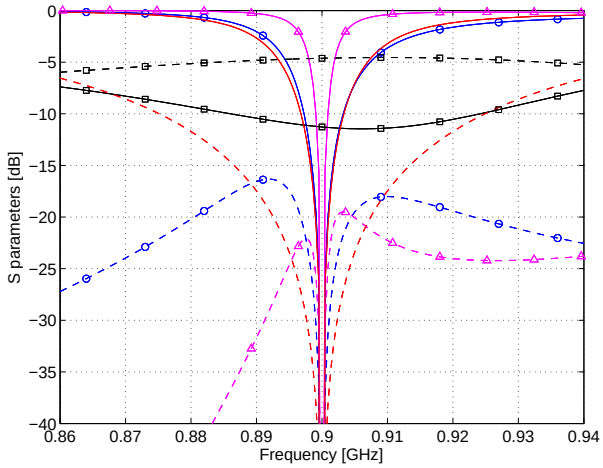

Fig. 4. Scattering parameters of two dipole arrays with and without parasitic scatterer: S'_{11} (-o-) and S'_{13} (-o-) for $L = 0.48\lambda$; S'_{11} (-△-) and S'_{13} (-△-) for $L = 0.38\lambda$; S_{odd} (——) and S_{even} (– –) are the odd and even modes of the MC matched dipoles; S_{11} (-□-) and S_{12} (-□-) are for two self-matched dipoles (*i.e.*, dipoles 1 and 2). No parasitic scatterer is used for the two dipoles with self- or MC match.

active elements. Monopole 3 is located at the center of the ground plane, whereas monopoles 1 and 2 are separated by 0.1λ and 0.05λ from monopole 3 along the positive y-axis, respectively (*i.e.*, $d = 0.1\lambda$). The ground plane of the monopole has the surface dimensions of 330 mm × 250 mm, and it is made from FR4 material of thickness 1.55 mm, with a thin copper coating on the underside of thickness 35 μm. The dielectric constant and loss tangent of the FR4 material at 900 MHz is 4.4 and 0.02, respectively. The copper-coated FR4 ground plane is used due to it being relatively lightweight and more rigid than pure copper ground plane of comparable thickness. The monopole conductors are made from cylindrical copper wires of 2 mm in diameter. Each of the two matching circuits, which is connected to the feeding end of the copper conductor, is printed on a PTFE printed circuit board (PCB) as transmission lines and open-circuited stubs. The PTFE PCB has a thickness of 0.8 mm and a copper layer of 35 μm. At 900 MHz, The PTFE material has a dielectric constant of 2.53 and a loss tangent of 0.0015.

The design procedure listed in Section II-A is applied to the simulation model of the monopole array setup. The simulation results of the monopole setup are obtained using the time-domain solver of CST Microwave Studio. For convenience of tuning, we apply distributed elements for both the reactive load at the parasitic element and the matching circuits at the active antennas. In particular, an open-circuited transmission line on a PCB is used as the reactive load and the matching circuits consist of transmission lines and single open-circuited stubs. These circuits are incorporated into the antenna simulation through circuit co-simulation in CST Design Studio. For the experimental verification, the scattering parameters of the fabricated monopole array (with the corresponding distributed decoupling and matching circuits attached) are measured with a two-port vector network analyzer and the radiation patterns are measured in a Satimo Stargate-64 measurement facility.

As in the case of dipoles, two reactance load solutions

can be found for perfect decoupling. However, we focus on the solution giving the larger bandwidth. The scattering parameters of the decoupled (and matched) active monopoles from simulation and measurement are given in Fig. 6. As can be seen, the simulation and measurement results are in good agreement with each other. Due to higher ohmic losses in practice than in simulation, the bandwidths of the measured cases are slightly larger than the simulated ones. Practical tuning likewise limits the exact reproduction of the isolation parameter.

The simulated and measured radiation patterns of the decoupled active elements are shown in Fig. 7. Again, the simulated and measured results are in good agreement. It is noted that the simulated E_ϕ component of the $\phi = 90°$ plane in Figs. 7(e) and 7(f) is not visible, since it is not within the given range of pattern magnitudes. In addition, the simulated patterns of the two active elements exhibit non-exact mirror symmetry, and this is because the center of the array is slightly displaced (*i.e.*, by 0.05λ) from the center of the ground plane. As can be expected from the linearly polarized monopoles, the E_θ component is dominant in the radiation patterns. Both $\theta = 90°$ and $\phi = 90°$ planes reveal that the maximum gains of the two patterns point away from each other, towards the array endfires ($\phi = 90°$ or $270°$), at a elevated angle of $\theta = 60°$. The directivity of the patterns is about 7.5 dBi, which is significantly higher than that of a single monopole. This confirms that angle diversity is strongly utilized in this setup. The simulated and measured pattern correlation, assuming a 3D uniform angular power spectrum (APS), is around 0.05 and 0.02, respectively. In the ideal case of a lossless setup, perfect decoupling and matching in the 3D uniform APS will lead to zero pattern correlation [7], [45]. The slight discrepancies between the theoretical zero correlation and the small correlation values in the simulated and measured cases are attributed to the presence of some losses and that it is difficult to practically obtain zero correlation.

The tolerance of efficiency measurement in the Satimo facility at 900 MHz is specified to be 0.5 dB. The simulated efficiencies of the parasitic decoupled monopoles are close to 100%, whereas the measured efficiencies are about 70%. The discrepancy is the primarily the result of imperfect fabrication of the antenna structure and the matching circuits, where the design of the experimental setup emphasizes flexibility rather than precise construction (*e.g.*, monopoles of different antenna spacing d can be easily achieved on the same ground plane). As a reference, the measured efficiency of a single monopole on the same ground plane is about 80%, which is within the tolerance range of the decoupled monopoles' efficiencies.

In contrast, for the same antenna spacing of $d = 0.1\lambda$ for the two-monopole setup which applies the MC match based on hybrid $180°$ coupler, the measured even and odd mode efficiencies at the center frequency are 75% and under 30%, respectively [13]. These efficiency values are for matching the even and odd mode outputs of the hybrid coupler with transmission lines and single open-circuited stubs (*i.e.*, the narrowband matching solution). Recall that similar matching elements are used to match the parasitic decoupled monopole ports. Comparing the achieved measured efficiency with parasitic decoupling and MC match, the parasitic decoupling approach is superior in terms of both average efficiency and balance of branch power.

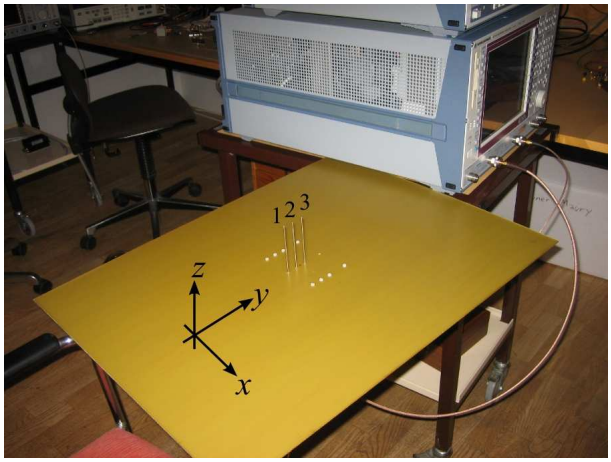

Fig. 5. Monopole uniform linear array of three elements, with the coordinate system used in the radiation pattern measurement.

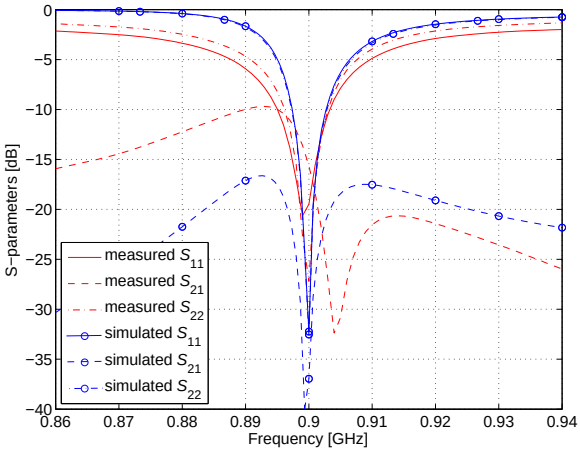

Fig. 6. Simulated and measured scattering parameters for active monopole antennas 1 and 3.

IV. Further Insights and Practical Aspects

A. Number of Antennas

For future systems, it is most realistic to first consider arrays with only two elements, though an extension of our proposed decoupling technique to the use of more elements is possible.

The technique will work for the case of three parallel dipoles (dipoles 1 to 3) in a uniform triangular array (UTA) arrangement, where one parasitic scatterer (dipole 4) in their centroid is able to decouple the triangular array for any separation distance between the active antennas. Applying the same approach from Section II-A in deriving (6) for decoupling two active antennas, and assuming that the active dipoles are identical, the corresponding expression for this three-dipole case is given by $Z_{\rm L} = Z_{14}^2/Z_{12} - Z_{44}$. For dipoles with a diameter of 2 mm and antenna spacing of $d = 0.1\lambda$ among the active dipoles, the scattering parameters as calculated using the MoM scripts from [42] for two UTA cases (*i.e.*, with and

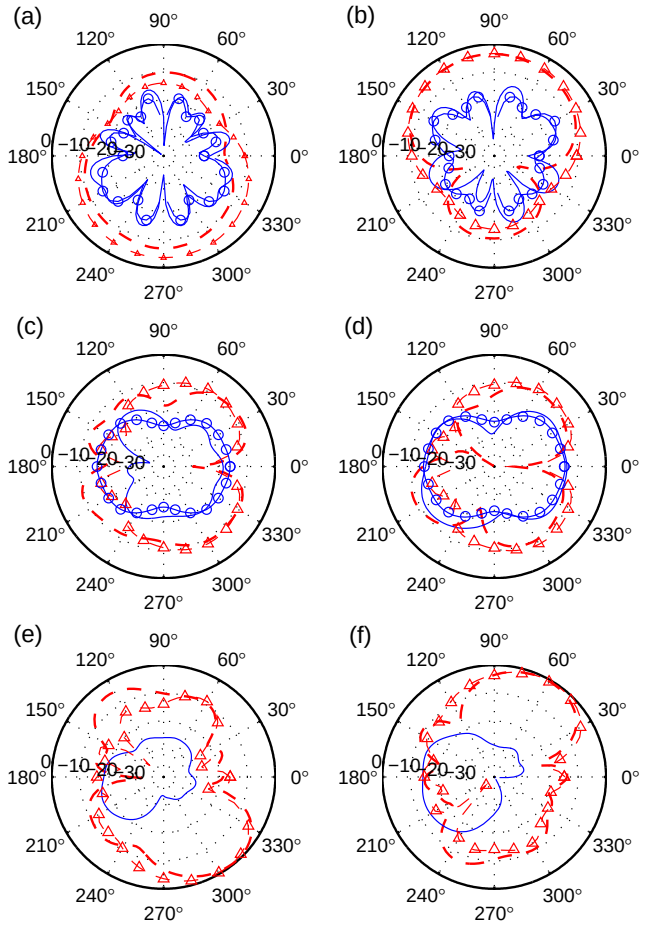

Fig. 7. Radiation patterns (dB) in the $\theta = 90°$ plane for (a) antenna 1 and (b) antenna 3, $\phi = 0°$ plane for (c) antenna 1 and (d) antenna 3, $\phi = 90°$ plane for (e) antenna 1 and (f) antenna 3: Simulated E_θ(—△—), measured E_θ,(- - -), simulated E_ϕ (—○—), measured E_ϕ (——). The coordinate system for the antenna system is given in Fig. 5. The pattern of each antenna is normalized by its maximum gain.

without a parasitic dipole at the centroid) are illustrated in Fig. 8. As before, the self-impedance match and half-wavelength dipoles are used for the reference case without the parasitic dipole. As can be seen, perfect decoupling is achieved at the center frequency when the reactively loaded parasitic dipole is applied, whereas the no-parasitic case has a high coupling coefficient of -7.5 dB between a given antenna and each of its two adjacent antennas. Nonetheless, as in the case of two-element arrays, decreasing the separation distance will result in a smaller bandwidth for the decoupled antennas. The reason that the decoupling technique applies directly to the UTA case is that the symmetry of the array structure ensures that the coupling between any (active) antenna pair is equal.

For three-element arrays of non-triangular arrangements, the inherent asymmetry in the array structure introduces different levels of coupling between different pairs of antennas, which complicates the design of parasitic scatterer(s) for perfect decoupling. However, the performance of multiple antenna systems is usually limited by pair(s) of antennas with the smallest antenna separation distance, such as for the case of uniform linear arrays of three or more elements. Therefore,

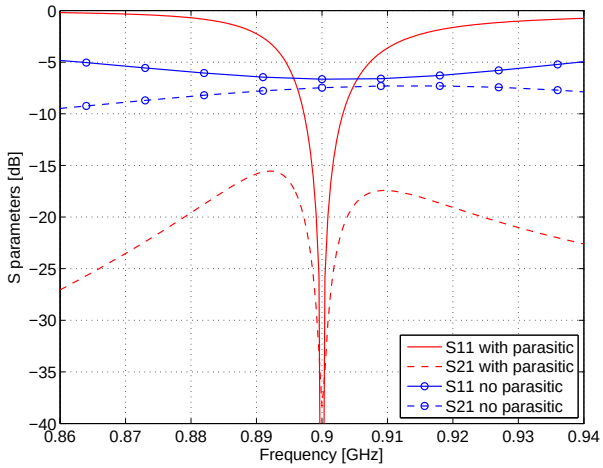

Fig. 8. Simulated scattering parameters for the UTA, with and without the reactively loaded parasitic scatterer. Due to symmetry $S_{11} = S_{22} = S_{33}$ and $S_{21} = S_{31} = S_{32}$, due to reciprocity.

decoupling the antenna pairs with the most severe coupling level can provide an approximate solution.

B. Application in Compact Terminals

One important application of decoupling techniques is in achieving good performance for mobile terminals with closely spaced antennas [6], [16]–[19]. Limited available space, multiple-band operation and the need for co-existence with other device components complicate the decoupling task significantly. Preliminary simulation results confirm that the proposed parasitic decoupling technique can perfectly decouple dual-PIFA and dual-monopole antennas at 900 MHz for a 40 mm × 100 mm ground plane, where the two active and one parasitic antennas are placed at the two short edges and the center of the ground plane, respectively.

C. MIMO Performance

It is known that a lossless decoupled and well matched receive array is optimum not only from the viewpoint of maximum power transfer from the antennas to the loads [9], it also facilitates zero correlation in the 3D uniform APS [7], [45]. In fact, the decoupled array is likewise superior in received power and correlation performance to coupled array in other propagation environments [41]. Since MIMO performance measured in terms of either capacity or diversity gain is a function of correlation, branch power imbalance and available power, arrays which are decoupled by any (lossless) method will in general result in a better MIMO performance as well (see *e.g.*, [6], [9], [46]).

As an example, we consider the MIMO capacity for the lossless dipoles in Section II at the center frequency. For a $M \times M$ MIMO channel $\mathbf{H}$, the instantaneous channel capacity with equal transmit power allocation can be expressed as [47]

$$C = \log_2 \det\left(\mathbf{I}_M + \frac{\rho}{M}\mathbf{H}\mathbf{H}^H\right), \qquad (11)$$

where ρ is the reference SNR and $\mathbf{I}_M$ is the $M \times M$ identity matrix. Since the interest here is in antenna design, the reference propagation environment of independent and identically

distributed (IID) Rayleigh fading channel $\mathbf{H}_{\rm w}$ is assumed, *i.e.*, the entries of $\mathbf{H}_{\rm w}$ are zero mean circularly symmetric complex Gaussian random variables. Without loss of generality, the case of receive antennas is examined. Then, the MIMO channel is given by

$$\mathbf{H} = \mathbf{R}^{\frac{1}{2}}\mathbf{H}_w, \tag{12}$$

where $\mathbf{R}$ is the receive correlation matrix, which fully represents the effects of the antennas on the channel, *i.e.*, it characterizes the efficiency, efficiency imbalance and correlation among the receive antennas. In particular,

$$\mathbf{R} = \mathbf{\Lambda}^{\frac{1}{2}}\bar{\mathbf{R}}\mathbf{\Lambda}^{\frac{1}{2}}, \tag{13}$$

where $\bar{\mathbf{R}}$ is a normalized correlation matrix whose diagonal elements are 1 and the (i,j)th $(i \neq j)$ element $\bar{\mathbf{R}}(i,j)$ denotes the complex correlation coefficient between the 3D radiation patterns of the ith and jth antenna ports. $\mathbf{\Lambda}$ denotes a diagonal matrix given by

$$\mathbf{\Lambda} = \mathrm{diag}[\eta_1, \eta_2, \cdots, \eta_M], \tag{14}$$

where η_i is the total effficiency of the ith antenna.

The correlation between the active antennas that has been decoupled with parasitic scatterer and matched to 50Ω is zero and the total efficiency of each antenna is 100%. This means that $\mathbf{R} = \mathbf{I}_M$ and the MIMO capacity is the same as that of the IID Rayleigh channel. For $\rho = 20$ dB and 10,000 Monte Carlo realizations of the $\mathbf{H}$, the ergodic capacity $\mathrm{E}(C)$ is 11.3 bits per second per Hertz (bits/s/Hz). In comparison, the correlation and total efficiency of the reference case with self-impedance match are 0.55 and 58%, respectively. This translates to an ergodic capacity of 9.4 bits/s/Hz. Thus, the proposed decoupling procedure gives an overall gain in capacity of 2 bits/s/Hz.

On the other hand, as also pointed out in Section II, the bandwidth of the decoupled array can be significantly smaller than that of a widely spaced array, depending on the antenna spacing [7]. This implies that at a very small antenna separation, the benefit of decoupling will be small, if the operating bandwidth significantly exceeds the achieved antenna bandwidth.

D. Shielded Zone

As can be seen in the pattern plots in Fig. 7, the shielding effect of the parasitic antenna ensures that the radiation of the active antennas is directed away from each other. However, the shielding effect is not only limited to far-field beamforming between the excited antenna and the parasitic element. Indeed, since decoupling is a near-field phenonmenon, one can expect that there is a quiet zone within the shielded region, as can be seen in the simulated total electric field distribution along the center region of the large ground plane in Fig. 9. In Fig. 9, active monopole antenna 1 is removed and the total electric field is taken at a height of 5 mm above the ground plane. As can be observed, the field at the former location of antenna 1 is over 10 dB lower than the value in the immediate vicinity of the excited antenna 3.

Moreover, due to the decoupling phenomenon, removing one of the two active antennas will only marginally affect the impedance and radiation characteristics of the other active antenna. This is confirmed in both simulations and measurements, *i.e.*, the remaining antenna gives similar reflection coefficient and radiation pattern as those shown in Figs. 6 and 7, respectively.

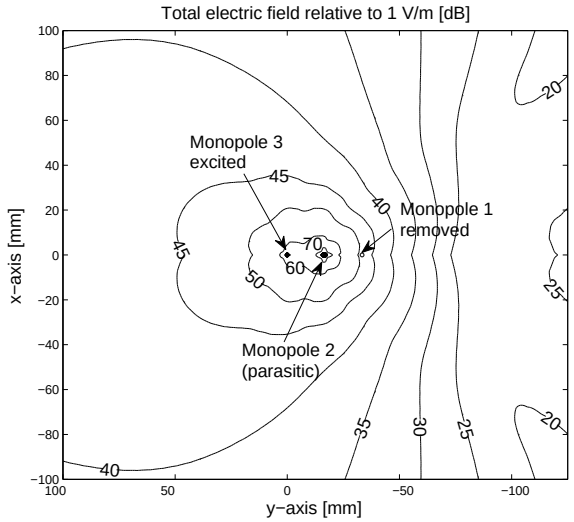

Fig. 9. Contour plot of the simulated total electric field (in dB) 5 mm above the ground plane when active monopole antenna 1 is removed. The center of the ground plane is at the origin and the coordinate system is shown in Fig. 5. The field is shown for only the center region of the ground plane.

V. Conclusions

This paper takes up the task of decoupling closely coupled antennas with parasitic scatterers. The main intention is to provide the theoretical insights into the approach, which can be applied to two arbitrary coupled antennas for an arbitrary spacing. Example applications on reference antenna arrays of closely spaced dipoles or monopoles illustrate the procedure and its effectiveness. Preliminary results confirm that the approach extends readily into more practical antenna elements, such as those used in mobile terminals. However, the ability of the parasitic scatterer approach to support multiband operation and its robustness to user effects are interesting subjects for future studies.

Acknowledgment

The authors would like to thank Mr. L. Hedenstjärna of the Department of Electrical and Information Technology, Lund University, for fabricating the antennas and matching circuits.

References

[1] B. K. Lau and J. B. Andersen, "Unleashing multiple antenna systems in compact terminal devices," in *Int. Workshop Antenna Technol. (IWAT2009)*, Santa Monica, CA, USA, Mar. 2-4, 2009.

[2] ——, "Antenna system and method of providing an antenna system," *Swedish Patent Application (No. 0702307-0)*, Oct. 2007.

[3] H. Krim and M. Viberg, "Two decades of array signal processing research: the parametric approach," *IEEE Signal Process. Mag.*, vol. 13, no. 4, pp. 67–94, Jul. 1996.

[4] S. Andersson, B. Hagerman, H. Dam, U. Forssï¿½n, J. Karlsson, F. Kronestedt, S. Mazur, and K. J. Molnar, "Adaptive antennas for GSM and TDMA systems," *IEEE Personal Commun. Mag.*, vol. 6, no. 3, pp. 74–86, Jun. 1999.

[5] E. Dahlman, S. Parkvall, and J. Sköld, *3G Evolution: HSPA and LTE for Mobile Broadband*. London: Academic Press, 2008.

[6] B. K. Lau, "Multiple antenna terminals," in *MIMO: From Theory to Implementation*, C. Oestges, A. Sibille, and A. Zanella, Eds. San Diego: Academic Press, 2011.

[7] B. K. Lau, J. B. Andersen, G. Kristensson, and A. F. Molisch, "Impact of matching network on bandwidth of compact antenna arrays," *IEEE Trans. Antennas Propag.*, vol. 54, no. 11, pp. 3225–3238, Nov. 2006.

[8] J. B. Andersen and H. H. Rasmussen, "Decoupling and descattering networks for antennas," *IEEE Trans. Antennas Propag.*, vol. AP-24, no. 6, pp. 841–846, Nov. 1976.

[9] J. W. Wallace and M. A. Jensen, "Mutual coupling in MIMO wireless systems: a rigorous network theory analysis," *IEEE Trans. Wireless Commun.*, vol. 3, no. 4, pp. 1317–1325, Jul. 2004.

[10] S. Dossche, S. Blanch, and J. Romeu, "Optimum antenna matching to minimise signal correlation on a two-port antenna diversity system," *Elect. Lett.*, vol. 40, no. 19, pp. 1164–1165, Sep. 16, 2004.

[11] ——, "Decorrelation of a closely spaced four element antenna array," in *IEEE Antenna Propagat. Soc. Int. Symp.*, vol. 1B, Washington, DC, USA, Jul. 3–8, 2005, pp. 803–806.

[12] S. Dossche, J. Rodriguez, L. Jofre, S. Blanch, and J. Romeu, "Decoupling of a two-element switched dual band patch antenna for optimum MIMO capacity," in *IEEE Antenna Propagat. Soc. Int. Symp.*, Albuquerque, NM, USA, Jul. 2006, pp. 325–328.

[13] C. Volmer, M. Sengul, J. Weber, R. Stephan, and M. A. Hein, "Broadband decoupling and matching of a superdirective two-port antenna array," *IEEE Antennas Wireless Propag. Lett.*, vol. 7, pp. 613–616, 2008.

[14] C. Volmer, J. Weber, R. Stephan, K. Blau, and M. A. Hein, "An eigen-analysis of compact antenna arrays and its application to port decoupling," *IEEE Trans. Antennas Propag.*, vol. 56, no. 2, pp. 360–370, Feb. 2008.

[15] C. Volmer, J. Weber, R. Stephan, , and M. A. Hein, "Mutual coupling in multi-antenna systems: figures-of-merit and practical verification," in *Europ. Conf. Antennas Propagat. (EUCAP2006)*, Berlin, Germany, Mar. 23-27, 2009.

[16] C. Y. Chiu, C. H. Cheng, R. D. Murch, and C. R. Rowell, "Reduction of mutual coupling between closely-packed antenna elements," *IEEE Trans. Antennas Propag.*, vol. 55, no. 6, pp. 1732–1738, Jun. 2007.

[17] Y. Gao, X. Chen, Z. Ying, and C. Parini, "Design and performance investigation of a dual-element PIFA array at 2.5 ghz for MIMO terminal," *IEEE Trans. Antennas Propag.*, vol. 55, no. 12, pp. 3433–3441, Dec. 2007.

[18] A. Diallo, C. Luxey, P. Le Thuc, R. Staraj, and G. Kossiavas, "Enhanced two-antenna structures for universal mobile telecommunications system diversity terminals," *IET Proc. Microw. Antennas Propagat.*, vol. 2, no. 1, pp. 93–101, Feb. 2008.

[19] C. Diallo, A. Luxey, R. Le Thuc, P. Staraj, and G. Kossiavas, "Diversity performance of multiantenna systems for UMTS cellular phones in different propagation environments," *Int. J. Antennas Propagat.*, 2008.

[20] A. C. K. Mak, C. R. Rowell, and R. D. Murch, "Isolation enhancement between two closely packed antennas," *IEEE Trans. Antennas Propag.*, vol. 56, no. 11, pp. 3411–3419, Nov. 2008.

[21] P. J. Ferrer, J. M. Gonzalez-Arbesu, and J. Romeu, "Decorrelation of two closely spaced antennas with a metamaterial amc surface," *Microwave and Optical Technology Lett.*, vol. 50, no. 5, pp. 1414–1417, May 2008.

[22] S. Hong, K. Chung, J. Lee, S. Jung, S. Lee, and J. Choi, "Design of a diversity antenna with stubs for UWB applications," *Microwave and Optical Technology Lett.*, vol. 50, no. 5, pp. 1352–1356, May 2008.

[23] A. Abe, N. Michishita, Y. Yamada, J. Muramatsu, T. Watanabe, and K. Sato, "Mutual coupling reduction between two dipole antennas with parasitic elements composed of composite right-/left-handed transmission lines," in *Int. Workshop Antenna Technol. (IWAT2009)*, Santa Monica, CA, USA, Mar. 2009.

[24] T. Michalski, V. Wienstroer, and R. Kronberger, "Beam forming capabilities of smart antennas on mobile terminal," in *Europ. Conf. Antennas Propagat. (EUCAP2009)*, Berlin, Germany, Mar. 23-27, 2009.

[25] S. Zhang, Z. Ying, J. Xiong, and S. He, "Ultrawideband MIMO/diversity antennas with a tree-like structure to enhance wideband isolation," *IEEE Antennas Wireless Propag. Lett.*, vol. 8, pp. 1279–1282, 2009.

[26] R. F. Harrington, "Reactively controlled directive arrays," *IEEE Trans. Antennas Propag.*, vol. 26, no. 3, pp. 390–395, May 1978.

[27] R. M. T. Milne, "A small adaptive array antenna for mobile communications," in *Proc. IEEE Antennas Propagat. Soc. Int. Symp.*, Vancouver, Canada, Jun. 17-21, 1985, pp. 797–800.

[28] N. L. Scott, M. O. Leonard-Taylor, and R. G. Vaughan, "Diversity gain from a single-port adaptive antenna using switched parasitic elements illustrated with a wire and monopole prototype," *IEEE Trans. Antennas Propag.*, vol. 47, no. 6, pp. 1066–1070, Jun. 1999.

[29] R. Schlub, D. V. Thiel, J. W. Lu, and S. G. O'Keefe, "Dual-band six-element switched parasitic array for smart antenna cellular communications systems," *Elect. Lett.*, vol. 36, no. 16, pp. 1342–1343, Aug. 3, 2000.

[30] P. Jarmuszewski, Y. Qi, and A. D. Stevenson, "Antenna with near-field radiation control," *Canadian Patent No. 2,414,124 A1*, Sep. 12, 2004.

[31] K. Sato and T. Amano, "Improvements of impedance and radiation performances with a parasitic element for mobile phone," in *Proc. IEEE Antennas Propagat. Soc. Int. Symp.*, San Diego, CA, Jul. 5-11, 2008.

[32] H. Nakano, R. Suzuki, and J. Yamauchi, "Low-profile inverted-f antenna with parasitic elements on an infinite ground plane," *IEE Proc. Microw. Antennas Propagat.*, vol. 145, no. 4, pp. 321–325, Aug. 1998.

[33] T. H. Tsai, H. T. Peng, and K. Shih, "Built-in multi-band mobile phone antenna assembly with coplanar patch antenna and loop antenna," *U.S. Patent Application Pub. No. 2004/0100410 A1*, May 27, 2004.

[34] G. Johnson and B. Newman, "Single or dual band parasitic antenna assembly," *US Patent No. 6,456,249 B1*, Sep. 24, 2002.

[35] K. Q. da Costa, V. A. Dmitriev, and M. N. Kawakatsu, "Enlarging the impedance matching bandwidth of wire and planar antennas using loop parasitic elements," in *Int. Workshop Antenna Technol. (IWAT2009)*, Santa Monica, CA, USA, Mar. 2009.

[36] J. C. Posluszny and R. C. Posluszny, "Parasitically coupled folded dipole multi-band antenna," *U.S. Patent Application Pub. No. 2006/0061515 A1*, Mar. 23, 2006.

[37] L. Li, Q. Chen, Q. Yuan, K. Sawaya, T. Maruyama, T. Furuno, and S. Uebayashi, "Novel broadband planar reflectarray with parasitic dipoles for wireless communication applications," *IEEE Antennas Wireless Propag. Lett.*, vol. 8, pp. 881–885, 2009.

[38] J. B. Andersen, J. O. Nielsen, G. F. Pedersen, G. Bauch, and M. Herdin, "Room electromagnetics," *IEEE Antennas Propag. Mag.*, vol. 49, no. 2, pp. 27–33, Apr. 2007.

[39] J. B. Andersen and B. K. Lau, "On closely coupled dipoles in a random field," *IEEE Antennas Wireless Propag. Lett.*, vol. 5, pp. 73–75, 2006.

[40] Y. Fei, Y. Fan, B. K. Lau, and J. S. Thompson, "Optimal single-port matching impedance for capacity maximization in compact MIMO arrays," *IEEE Trans. Antennas Propag.*, vol. 56, no. 11, pp. 3566–3575, Nov. 2008.

[41] M. A. Jensen and B. K. Lau, "Uncoupled matching for active and passive impedances of coupled arrays in MIMO systems," *IEEE Trans. Antennas Propag.*, vol. 58, no. 10, pp. 3336–3343, Oct. 2010.

[42] S. M. Makarov, *Antenna and EM Modeling with MATLAB*. New York: John Wiley and Sons, 2002.

[43] R. Vaughan and J. Bach Andersen, *Channels, Propagation And Antennas For Mobile Communications*. London: The IEE, 2003, pp. 511.

[44] D. M. Pozar, *Microwave Engineering, 3rd Ed*. Hoboken, NJ: John Wiley and Sons, 2005.

[45] S. Blanch, J. Romeu, and I. Corbella, "Exact representation of antenna system diversity performance from input parameter description," *Elect. Lett.*, vol. 39, no. 9, pp. 705–707, May 2003.

[46] J. W. Wallace and M. A. Jensen, "Termination-dependent diversity performance of coupled antennas: network theory analysis," *IEEE Trans. Antennas Propag.*, vol. 52, no. 1, pp. 98–105, Jan. 2004.

[47] A. Paulraj, R. Nabar, and D. Gore, *Introduction to Space-Time Wireless Communications*. Cambridge: Cambridge University Press, 2003.

Buon Kiong Lau (S'00-M'03-SM'07) obtained the Bachelor of Electrical and Electronic Engineering degree from the University of Western Australia, Australia and the Ph.D. degree from Curtin University of Technology, Australia, in 1998 and 2003, respectively. From 2003 to 2004, he was a Guest Research Fellow at the Department of Signal Processing, Blekinge Institute of Technology, Sweden. In 2004, he was appointed a Research Fellow at the Department of Electroscience, Lund University, Sweden. In 2007, he became an Assistant Professor at the Department of Electrical and Information Technology (formerly Department of Electroscience), Lund University, Sweden, where he is now an Associate Professor. During 2003, 2005 and 2007, he was also a Visiting Researcher at the Department of Applied Mathematics, Hong Kong Polytechnic University, China, Laboratory for Information and Decision Systems, Massachusetts Institute of Technology, USA, and Takada Laboratory, Tokyo Institute of Technology, Japan, respectively.

Dr Lau is an Associate Editor for the IEEE Transactions on Antennas and Propagation and a Guest Editor of the upcoming 2011 Special Issue on MIMO Technology for the same journal. He is a Co-chair of Subworking Group 2.2 on "Compact Antenna Systems for Terminals" (CAST) within EU COST Action 2100 and a Senior Member of the IEEE. Dr Lau's primary research interests are in various aspects of multiple antenna systems, particularly the interplay between traditionally separate disciplines of antennas, propagation channels and signal processing.

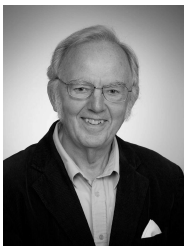

Jørgen Bach Andersen (M'68-SM'78-F'92-LF'02) received the M.Sc. and Dr.Techn. degrees from the Technical University of Denmark (DTU), Lyngby, Denmark, in 1961 and 1971, respectively. In 2003 he was awarded an honorary degree from Lund University, Sweden. From 1961 to 1973, he was with the Electromagnetics Institute, DTU and since 1973 he has been with Aalborg University, Aalborg, Denmark, where he is now a Professor Emeritus and Consultant. He was head of a research center, Center for Personal Communications, CPK, from 1993-2003.

He has been a Visiting Professor in Tucson, Arizona, Christchurch, New Zealand, Vienna, Austria, and Lund, Sweden. He has published widely on antennas, radio wave propagation, and communications, and has also worked on biological effects of electromagnetic systems. He has coauthored a book, 'Channels, Propagation and Antennas for Mobile Communications', IEE, 2003 with Rodney G. Vaughan. He was on the management committee for COST 231 and 259, a collaborative European program on mobile communications. He is Associate Editor of 'Antennas and Wireless Propagation Letters', and Co-Editor of a joint special issue of IEEE Transactions on Antennas and Propagation and Microwave Theory and Techniques on 'Multiple-Input Multiple-Output (MIMO) Technology'.

Professor Andersen is a former Vice President of the International Union of Radio Science (URSI) from which he was awarded the John Howard Dellinger Gold Medal in 2005.